ELSEVIER

Catalysis Today 63 (2000) 347–353

CATALYSIS TODAY

www.elsevier.com/locate/cattod

Effects of methane and oxygen on decomposition of nitrous oxide over metal oxide catalysts

Atsushi Satsuma [a,*], Hajime Maeshima [a], Kiyoshi Watanabe [a], Kenji Suzuki [a], Tadashi Hattori [b]

[a] *Department of Applied Chemistry, Graduate School of Engineering, Nagoya University, Furocho, Chikusa-ku, Nagoya 464-8603, Japan*
[b] *Research Center for Advanced Waste and Emission Management, Nagoya University, Chikusa-ku, Nagoya 464-8603, Japan*

Abstract

Catalytic activities of various metal oxides for decomposition of nitrous oxide were compared in the presence and absence of methane and oxygen, and the general rule in the effects of the coexisting gases was discussed. The reaction rates of nitrous oxide were well correlated to the heat of formation of metal oxide, i.e., a V-shaped relationship with a minimum at $-\Delta H_f^0$ around 450 kJ (O mol)$^{-1}$ was observed in N_2O decomposition in an inert gas. In the case of metal oxides having the heat of formation lower than 450 kJ (O mol)$^{-1}$, CuO, Co_3O_4, NiO, Fe_2O_3, SnO_2, In_2O_3, Cr_2O_3, the activities were strongly affected by the presence of methane and oxygen. On the other hand, the activities of TiO_2, Al_2O_3, La_2O_3, MgO and CaO were almost independent. The reaction rate of nitrous oxide was significantly enhanced by methane. The promotion effect of methane was attributed to the reduction of nitrous oxide with methane: $4N_2O + CH_4 \rightarrow 2N_2 + CO_2 + 2H_2O$. The activity was suppressed in the presence of oxygen on the metal oxides having lower heat of formation. On the basis of Langmuir–Hinshelwood mechanism, the effect of oxygen on nitrous oxide decomposition was rationalized with the strength of metal–oxygen bond.

Keywords: Decomposition; Nitrous oxide; Metal oxide catalysts; Catalytic activity

1. Introduction

Nitrous oxide (N_2O) is considered to be responsible for stratospheric ozone layer depletion and is thought to be responsible for "global warming" [1–3]. Catalytic removal of nitrous oxide from artificial sources, i.e., the manufacture of adipic acid [4], fluidized beds for combustion and automotive exhaust emissions, would be one of the possible solutions to protect our environment. Various types of catalysts have been reported to be active for the decomposition of nitrous oxide. Ion-exchanged zeolites, such as Co-, Cu-, Fe-, Rh- and Ru-exchanged ZSM-5 exhibit good performance in N_2O decomposition [5–12]. However, the catalytic activity on decomposition of nitrous oxide would be significantly affected by various coexisting gases, such as oxygen, water vapor, and hydrocarbons [10–12]. For example, although Ru-ZSM-5 is very active at low temperatures, it is significantly deactivated in the presence of excess oxygen [11]. Li and Armor [10] reported that the presence of oxygen appears to have no effect on N_2O decomposition on Co-ZSM-5, though N_2O conversion on Co-ZSM-5 substantially decreased in the presence of both methane and oxygen. We also reported that N_2O conversion in N_2O–CH_4–O_2 reaction over metal oxides is inhibited by excess oxygen, while only CaO exhibits high activity free from the inhibitory effect of oxygen [14].

* Corresponding author. Tel.: +81-52-789-4608; fax: +81-52-789-3193.
E-mail address: satsuma@apchem.nagoya-u.ac.jp (A. Satsuma).

0920-5861/00/$ – see front matter
PII: S0920-5861(00)00478-8

Table 1
Source, surface area and the heat of formation of oxide catalysts

Catalyst	Source	Surface area ($m^2\,g^{-1}$)	$-\Delta H_f^0$ (kJ (mol O)$^{-1}$)
Al_2O_3	JRC-ALO-1A, Japan reference catalyst	157	558.4
CaO	Commercially supplied (Kishida)	4.0	635.1
Co_3O_4	Thermal decomposition of cobalt acetate in O_2 at 1073 K	1.2	202.3
Cr_2O_3	Commercially supplied (Kishida)	2.4	380.0
CuO	Thermal decomposition of copper nitrate in air at 973 K	0.79	157.0
Fe_2O_3	Commercially supplied (Kanto)	9.2	274.7
In_2O_3	Commercially supplied (Mitsuwa)	6.8	308.6
La_2O_3	Commercially supplied (Kishida)	2.0	598.0
MgO	JRC-MGO-1, Japan reference catalyst	143	601.7
NiO	Commercially supplied (Kishida)	2.9	245.2
SnO_2	Commercially supplied (Mitsuwa)	4.6	290.5
TiO_2	JRC-TIO-4, Japan reference catalyst	26.2	470.0

Since the practical catalysts are usually composed of various types of elements, a general relationship between inhibitory effect of coexisting gases should be clarified for the catalyst design. In the present work, effects of methane and oxygen on N_2O conversion on various metal oxides are examined, and the general rule in the effects of these coexisting gases is discussed.

2. Experimental

Al_2O_3, CaO, Co_3O_4, Cr_2O_3, CuO, Fe_2O_3, In_2O_3, La_2O_3, MgO, NiO, SnO_2 and TiO_2 were used as metal oxide catalysts as listed in Table 1. All the catalysts were pressed and sieved in the range 28–48 mesh, and then calcined in flowing oxygen at 873 K for 3 h. A catalytic test was carried out in a conventional continuous flow apparatus at atmospheric pressure [13,14]. Before the test, the catalysts were calcined in flowing oxygen at 823 K for 1 h, in order to keep the catalysts in a highly oxidized state. In the catalytic runs without methane and oxygen, a mixture gas containing 1% N_2O diluted with He was fed to 0.2–3.0 g of a catalyst at a total flow rate of 100 cm^3(STP) min^{-1}. For all the catalysts, the ratio of produced N_2 and O_2 was equivalent to the stoichiometry ($N_2O \rightarrow N_2 + \frac{1}{2}O_2$), i.e., O/N_2 ratio was unity. In the runs with methane and oxygen, 1% CH_4 and 8% O_2 were added at the sacrifice of the equivalent amount of He, respectively. The catalytic run was at first started at 823 K, and after the confirmation of steady-state activity for more than 180 min, the reaction temperature was decreased stepwise. In order to compare the reaction rate under a nearly differential reaction condition, the catalytic runs were carried out at low N_2O conversion, below 30%, by varying catalyst weight.

3. Results and discussions

3.1. Changes of activity in presence of methane and oxygen

Fig. 1 shows examples of the temperature dependence of N_2O conversion in the presence and absence of methane and oxygen. The N_2O conversion on CuO became higher by the addition of methane into the feed gas. Since methane simultaneously converted to CO_2, the increase in the activity is due to the reduction of N_2O by methane. On the other hand, N_2O conversion on La_2O_3 decreased in the presence of methane, and a small amount of methane oxidized. In the presence of oxygen, nitrous oxide decomposition was suppressed both on CuO and La_2O_3. The suppression was larger on CuO. The significant decrease in the activity was also observed in Co_3O_4, NiO, Fe_2O_3, SnO_2, In_2O_3 and Cr_2O_3. From a periodic reaction of N_2O decomposition between the absence and presence of oxygen, it was confirmed that the inhibition is caused by reversible adsorption of oxygen onto surface sites. The conversion of N_2O was decreased by introduction of oxygen, and then become steady state. The activity was immediately recovered by removal of oxygen

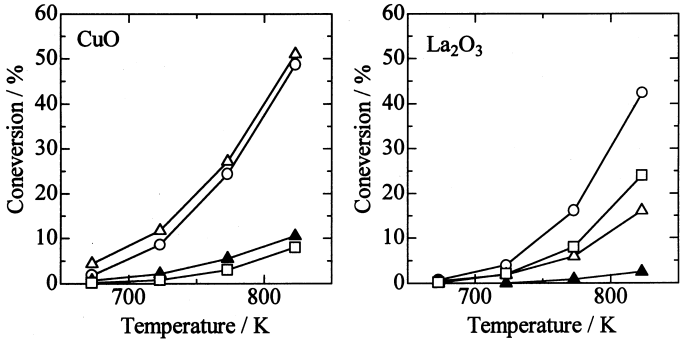

Fig. 1. Conversion of nitrous oxide in a stream of 1% N_2O diluted in He (open circles), 1% N_2O–1% CH_4 (open triangles), and 1% N_2O–8% O_2 (open squares) over CuO (left) and La_2O_3 (right). Closed triangles represent CH_4 conversion in N_2O–CH_4 reaction (closed triangles). Catalyst weight: 1 g.

from the feed gas. There was also no or small change in the activity of TiO_2, Al_2O_3, La_2O_3 and CaO.

The conversions of N_2O and methane in N_2O–CH_4 reaction were compared in Fig. 2. In the case of CuO, Cr_2O_3, NiO, Fe_2O_3, SnO_2 and In_2O_3, the ratio of N_2O conversion to methane conversion was along the stoichiometry of the selective reduction of N_2O by CH_4: $4N_2O + CH_4 \rightarrow 2N_2 + CO_2 + 2H_2O$. This indicates that the direct decomposition of nitrous oxide is predominant over these catalysts. In the case of Al_2O_3, CaO, Co_3O_4, La_2O_3, MgO and TiO_2, N_2O conversion exceeded the stoichiometric ratio, representing that both direct decomposition and selective reduction of N_2O simultaneously occurred on these catalysts.

Fig. 3 shows the correlation between reaction rates of N_2O in the presence and absence of methane. In the case of CuO, Cr_2O_3, NiO, Fe_2O_3, In_2O_3 and SnO_2, the rate of N_2O in the presence of methane was higher than in the absence of methane. As for the other metal oxides, the N_2O decomposition activity decreased or not much affected by the presence of methane.

In Fig. 4, the reaction rates of N_2O in the presence and absence of oxygen were compared. The reaction rates were significantly suppressed on CuO, Co_3O_4 and Cr_2O_3 in the presence of oxygen. On the other catalysts, the activity for N_2O decomposition was only slightly or not suppressed.

3.2. Dependence on the heat of formation of metal oxides

Fig. 5 summarized the effect of methane and oxygen on the reaction rate of N_2O as a function of the heat of

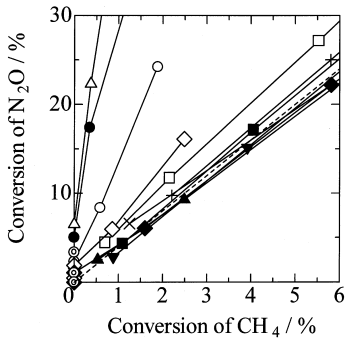

Fig. 2. Comparison between conversion of N_2O and CH_4 in N_2O–CH_4 reaction over Al_2O_3 (○), CaO (●), Co_3O_4 (△), Cr_2O_3 (▲), CuO (□), Fe_2O_3 (■), In_2O_3 (▼), La_2O_3 (◇), MgO (◆), NiO (+), SnO_2 (×), TiO_2 (◎).

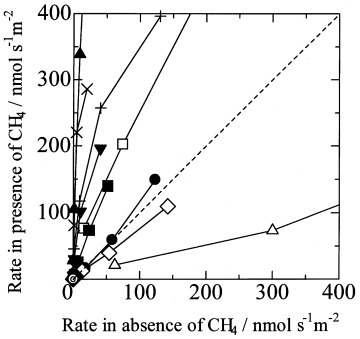

Fig. 3. Comparison of reaction rate of N_2O in the presence and absence of CH_4. For the symbols, see Fig. 2.

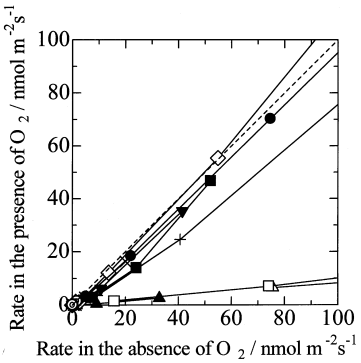

Fig. 4. Comparison of reaction rate of N_2O in the presence and absence of oxygen. For the symbols, see Fig. 2.

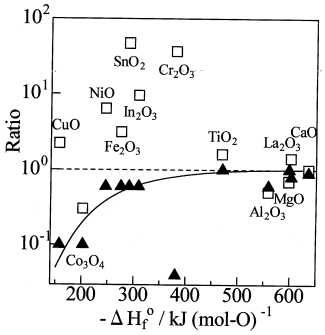

Fig. 6. Ratio of N_2O decomposition rate in a stream of N_2O diluted in He to N_2O–CH_4 reaction (open squares) and to N_2O–O_2 reaction (closed triangles) at 773 K as a function of heat of formation.

formation of oxides ($-\Delta H_f^0$) per lattice oxygen [15]. In the decomposition of N_2O in an inert gas (closed circles), a V-shaped relation was observed with a minimum reaction rate at around 450 kJ (O mol)$^{-1}$. This trend is the same as those reported by Vijh [16], suggesting N_2O decomposition activity can be correlated to the strength of metal–oxygen bond in oxide catalysts. In the presence of methane (open squares), the catalytic activity significantly increased at the descending branch, i.e., metal oxides having the heat of formation lower than 450 kJ (mol O)$^{-1}$. Co_3O_4 was only the exception. Conversions of N_2O and methane on these oxides indicate that the reduction of nitrous oxide with methane mainly proceeded as follows: $4N_2O + CH_4 \rightarrow 2N_2 + CO_2 + 2H_2O$. On the contrary to this, the catalytic activity over metal oxides having higher heat of formation, i.e., CaO, La_2O_3, MgO, Al_2O_3 and TiO_2, was not much affected by methane.

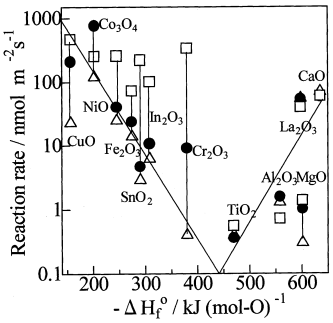

Fig. 5. Reaction rate of N_2O at 773 K in a stream of N_2O diluted in He (closed circles), N_2O–CH_4 (open squares), and N_2O–O_2 (open triangles) as a function of the heat of formation of metal oxides.

In the presence of oxygen, the changes in the activity were smaller than that of methane, however, the trend was also basically classified into two groups. Winter [17,18] also classified the effect of oxygen on various metal oxide catalysts into two types, i.e., no effect and retardation. His classification of metal oxides is essentially similar to our results, but the classification was not well correlated to catalyst properties in his report.

Fig. 6 shows the ratio of reaction rate of N_2O in the presence and absence of methane and oxygen. This figure represents gradual changes in the effects of methane and oxygen along with the heat of formation of metal oxides. The promotion by methane was higher at lower heat of formation, but the effect gradually decreased with increase in the heat of formation. The inhibitory effect of oxygen was also larger at lower heat of formation. These trends were also observed at the other temperatures. Since the heat of formation can be regarded as an indicator of metal–oxygen bond, the figure strongly suggests that the promotion by methane and inhibition by oxygen can be correlated to the strength of metal–oxygen bond.

3.3. Effect of methane

Kinetics of N_2O decomposition have been well studied [5,17–26]. Although various kinetic models are proposed so far, the reaction can be basically described as an adsorption of N_2O on the active center

followed by the decomposition of N_2O and desorption of oxygen. The reaction scheme can be well described with a simple Langmuir–Hinshelwood model derived by postulating quasi-equilibrated N_2O adsorption, a rate-determining N_2O decomposition step, and quasi-equilibrated desorption of O_2 [5,24–26]

$$N_2O + * \overset{K(N_2O)}{\rightleftharpoons} N_2O^* \quad (1)$$

$$N_2O^* \overset{k}{\rightarrow} N_2 + O^* \quad (2)$$

$$2O^* \overset{1/K(O_2)}{\rightleftharpoons} O_2 + 2^* \quad (3)$$

where * denotes a surface site. It is generally accepted that surface vacant sites, i.e., surface coordinatively unsaturated sites (CUS), are responsible for nitrous oxide decomposition [4,17,18]. Taking above Langmuir–Hinshelwood model into account, the volcano-type plot on N_2O decomposition in He can be correlated to the M–O bond strength as Vijh [16] claimed. In the descending branch of the V-shaped correlation, the activity decreases with increasing the strength of M–O bond. In the ascending branch of the V-shaped correlation, activity increases with increase in the M–O bond, indicating rate-determining step involves the formation of M–O bond.

In the presence of methane, the selective reduction of N_2O by methane also proceeds on some of the metal oxides as shown in Fig. 2.

$$4N_2O + CH_4 \rightarrow 2N_2 + CO_2 + 2H_2O \quad (4)$$

The selective reaction was predominant on the metal oxides at the descending branch of the V-shaped correlation. The selective reduction of N_2O by methane involves the removal of adsorbed oxygen on metal oxide surface sites.

$$4O\text{–}M + CH_4 \rightarrow []\text{–}M + CO_2 + 2H_2O \quad (5)$$

The symbol [ ]–M represents the vacant site on metal oxide surface. Thus, the increase in the activity by methane on the metal oxides at the descending branch can be attributed to the removal of adsorbed oxygen by the selective reduction of methane. The activity enhancement on the metal oxides having lower heat of formation should be due to the weaker M–O bond, which can be related to redox activity of metal oxides. On the contrary to this, the activity of metal oxides on the ascending branch of the V-shaped correlation, having no or weak redox activity, were not or slightly affected by the presence of methane.

As an exception, the catalytic activity of Co_3O_4 was suppressed in the presence of methane. Co_3O_4 also showed a unique character. The direct decomposition of N_2O was predominant than the selective reduction by methane as shown in Fig. 2. This unique catalytic property of Co_3O_4 may be correlated to the high activity of Co-ZSM-5 for N_2O decomposition reported by Li and Armor [10] and Andrade and coworkers [12]. It can be expected that the decrease in N_2O conversion on Co_3O_4 in the presence of methane is due to the adsorption of any molecules, such as carbonate, on surface site for direct decomposition of N_2O.

3.4. Effect of oxygen

The effect of oxygen can be rationalized by the kinetic equations based on Eqs. (1)–(3) after the following modification. Yamashita and Vannice [26] represented that the equilibrium constants of oxygen desorption, $K(O_2)$, is 1 or 2 orders higher than $K(N_2O)$ on manganese oxides. The transient kinetic study reported by Kobayashi and Kobayashi [22] showed that O_2 desorption is slower than that of N_2O desorption. Moreover, taking the excess amount of oxygen (8%) into account, the quasi-equilibrated N_2O adsorption step should be slower enough than oxygen desorption and can be neglected as the first approximation. Actually, a reversible suppression of the decomposition activity by the presence of excess oxygen indicates the significant contribution of Eq. (3). Thus, the kinetic model applicable to this work can be simplified in the following equations [13]:

$$N_2O + []\text{–}M \overset{k_1}{\rightarrow} O\text{–}M + N_2 \quad (6)$$

$$O\text{–}M \underset{k_3}{\overset{k_2}{\rightleftharpoons}} \frac{1}{2}O_2 + []\text{–}M \quad (7)$$

The rate of oxygen coverage on surface vacant sites, θ, can be described as follows:

$$\frac{d\theta}{dt} = k_1[N_2O](1-\theta) + k_3[O_2]^{1/2}(1-\theta) - k_2\theta \quad (8)$$

By using the steady-state approximation ($d\theta/dt = 0$), the oxygen coverage in the presence of oxygen can be indicated in Eq. (9).

$$\theta(\text{with } O_2) = \frac{(k_1/k_2)[N_2O] + (k_3/k_2)[O_2]^{1/2}}{1 + (k_1/k_2)[N_2O] + (k_3/k_2)[O_2]^{1/2}} \quad (9)$$

In the absence of oxygen, the coverage of oxygen is,

$$\theta(\text{without } O_2) = \frac{(k_1/k_2)[N_2O]}{1 + (k_1/k_2)[N_2O]} \quad (10)$$

From Eqs. (9) and (10), the relative coverage of oxygen in the presence and absence of oxygen is as follows:

$$\frac{\theta(\text{with } O_2)}{\theta(\text{without } O_2)} = \frac{(1 + (k_1/k_2)[N_2O])((k_1/k_2)[N_2O] + (k_3/k_2)[O_2]^{1/2})}{(k_1/k_2)[N_2O](1 + (k_1/k_2)[N_2O] + (k_3/k_2)[O_2]^{1/2})} \quad (11)$$

The reaction rate of N_2O decomposition would correlate well with the number of uncovered surface sites. At the descending branch of the V-shaped correlation, the lower heat of formation ($-\Delta H_f^0 < 450\,\text{kJ (mol O)}^{-1}$) means the lower strength of metal–oxygen bond, which results in the smaller rate constants of oxygen adsorption (k_1, k_3). Assuming an extreme case, i.e., extrapolation of k_1/k_2 and k_3/k_2 in Eq. (11) to zero, the change in oxygen coverage will be above unity.

$$\lim_{k_1/k_2,\, k_3/k_2 \to 0} \frac{\theta(\text{with } O_2)}{\theta(\text{without } O_2)} = 1 + \frac{k_3[O_2]}{k_1[N_2O]} > 1 \quad (12)$$

This equation indicates the higher coverage of active sites with oxygen during N_2O decomposition, which should lead to the decrease in the active sites and thus the strong inhibition of decomposition activity.

In the absence of oxygen, smaller k_1 and k_3 result in the smaller coverage of oxygen as given by the equation

$$\lim_{k_1/k_2,\, k_3/k_2 \to 0} \theta(\text{without } O_2) = 0 \quad (13)$$

In other words, this means the higher exposure of active sites during the N_2O decomposition on metal oxides having lower heat of formation, such as CuO and Co_3O_4. This should be the reason why the increase in activity of N_2O decomposition in an inert gas with the decrease in the heat of formation as shown in the closed circles in Fig. 5.

Only the exception was Cr_2O_3. The activity in the presence of oxygen was much smaller than expected from its heat of formation. This exception can be rationalized by assuming higher oxidation state of chromium oxide surface. If Cr_2O_3 is oxidized to CrO_3, of which the heat of formation is $197\,\text{kJ (mol O)}^{-1}$, the degree of inhibition should be on a level with those of CuO and Co_3O_4. It is reasonable that Cr_2O_3 was oxidized during N_2O decomposition because of the highly oxidized atmosphere. Since the bulk phase did not changed after the reaction, the oxidation would be limited only to the external surface.

At the ascending branch, i.e., the metal oxides having higher heat of formation ($-\Delta H_f^0 > 450\,\text{kJ (mol O)}^{-1}$), the rate constants of oxygen adsorption (k_1, k_2) should be larger because of the strong metal–oxygen bond. Assuming an extreme case, i.e., k_1/k_2 and k_3/k_2 are infinity, the ratio of oxygen coverage is nearly equal to unity.

$$\lim_{k_1/k_2,\, k_3/k_2 \to \infty} \frac{\theta(\text{with } O_2)}{\theta(\text{without } O_2)} = 1 \quad (14)$$

Eq. (14) indicates that the coverage is independent of the presence of oxygen. Thus, the activity for N_2O decomposition was not or slightly decreased over TiO_2, Al_2O_3, MgO, La_2O_3, and CaO.

One may expect that above explanation is strange because the catalysts highly covered by oxygen exhibited moderate activity for the decomposition. Actually, Eq. (15) indicates that some active sites are already poisoned even in the absence of oxygen.

$$\lim_{k_1/k_2,\, k_3/k_2 \to \infty} \theta(\text{without } O_2) = \lim_{k_1/k_2,\, k_3/k_2 \to \infty} \frac{(k_1/k_2)[N_2O]}{1 + (k_1/k_2)[N_2O]} = 1 \quad (15)$$

One of the possible reasons is the presence of different types of surface sites, i.e., those strongly poisoned by oxygen and those are not affected by oxygen. We previously reported that the catalytic activity of CaO for N_2O decomposition is strongly depend on surface geometric structure [27]. Highly unsaturated sites are extremely active but readily poisoned by oxygen. On the other hand, moderate and poor unsaturated sites, such as plane sites, are responsible for continuous catalytic decomposition of nitrous oxide. The presence of different types of active sites may be the reason

for the high activity of CaO and La_2O_3. Although a part of surface sites are readily poisoned irrespective of gaseous oxygen, another part of surface sites would be active even in the presence of oxygen.

4. Conclusion

The effects of methane and oxygen on N_2O decomposition were investigated by using various metal oxide catalysts. The reaction rate of N_2O decomposition in an inert gas shows a V-shaped correlation with the heat of formation of metal oxides. The effects of methane and oxygen were significant at the descending branch of the correlation, i.e., metal oxides having lower heat of formation. The enhancement of the activity in the presence of methane was attributed to the selective reduction of N_2O by methane. The higher redox activity of these oxides is profitable for the selective reduction. On the contrary to this, these oxides were significantly suppressed by the presence of oxygen. The larger suppression on N_2O decomposition in the presence of oxygen was rationalized on the basis of Langmir–Hinshelwood mechanism and the strength of metal–oxygen bond.

References

[1] R.E. Dickinson, R.J. Cicerone, Nature 319 (1986) 109.
[2] N. Arai, Inst. Energy 67 (1994) 61.
[3] J.F. Andrews, P. Brimblecombe, T.D. Jickells, P.S. Liss, An Introduction to Environmental Chemistry, Blackwell Science, Oxford, 1996, p. 181.
[4] M.H. Thiemens, W.C. Trogler, Science 251 (1991) 932.
[5] F. Kapteijn, J. Rodriguez-Mirasol, J.A. Moulijn, Appl. Catal. B 9 (1996) 25 and references cited there in.
[6] B.W. Riley, J.R. Richmond, Catal. Today 17 (1993) 277.
[7] J. Leglise, J.O. Petunchi, K.W. Hall, J. Catal. 86 (1984) 392.
[8] Y. Li, J.N. Armor, Appl. Catal. B 1 (1992) L21.
[9] M. Tabata, H. Hamada, Y. Kindaichi, M. Sasaki, T. Ito, Chem. Express 7 (1992) 77.
[10] Y. Li, J.N. Armor, Appl. Catal. B 3 (1993) 55.
[11] Y. Chang, J.G. McCarty, E.D. Wachsman, Appl. Catal. B 6 (1995) 21.
[12] R.S. da Curz, A.J.S. Mascarenhas, H.M.C. Andrade, App. Catal. B 18 (1998) 223.
[13] A. Satsuma, H. Maeshima, K. Watanabe, T. Hattori, Energy Convs. Mgmt., in press.
[14] H. Muramatsu, K. Tokura, T. Mori, R. Akahori, K. Watanabe, A. Satsuma, T. Hattori, Y. Murakami, Energy Convs. Mgmt. 38 (1997) 1399.
[15] Chemical Society of Japan (Ed.), Kagaku-Binran (Handbook of Chemistry), 3rd Edition, Vol. II-312, Maruzen, Tokyo, 1984.
[16] A.K. Vijh, J. Catal. 31 (1973) 51.
[17] E.S.R. Winter, J. Catal. 19 (1970) 32.
[18] E.S.R. Winter, J. Catal. 34 (1974) 431, 440.
[19] L. Rheaume, G.P. Arravano, J. Phys. Chem. 63 (1959) 264.
[20] K. Tanaka, A. Ozaki, J. Catal. 40 (1967) 421.
[21] A. Cimino, V. Indovina, J. Catal. 17 (1970) 54.
[22] H. Kobayashi, M. Kobayashi, Catal. Rev. -Sci. Eng. 10 (1974) 139.
[23] C.S. Sway, J. Christopher, Catal. Rev. -Sci. Eng. 34 (1992) 409.
[24] M.A. Vannice, S.H. Hyun, B. Kalpakci, W.C. Liauh, J. Catal. 56 (1979) 358.
[25] A. Vannice, A.B. Walters, X. Zhang, J. Catal. 159 (1996) 119.
[26] T. Yamashita, A. Vannice, J. Catal. 161 (1996) 254.
[27] A. Satsuma, R. Akahori, M. Kato, S. Komai, H. Yoshida, T. Hattori, J. Mol. Catal. A 155 (2000) 81.